Innovative Approach to the Catalytic Effects of Oxide Glasses and Glass-Ceramics on the Thermal Decomposition of Fatty Acids

Sara Marijan,[a] Petr Mošner,[b] Ladislav Koudelka,[b] Željko Skoko,[c] Luka Pavić,[a*] Jana Pisk[d,*]

[a]*Division of Materials Chemistry, Ruđer Bošković Institute, Bijenička 54, HR-10000 Zagreb, Croatia*
[b]*Department of General and Inorganic Chemistry, Faculty of Chemical Technology, University of Pardubice, 53210 Pardubice, Czech Republic*
[c]*Department of Physics, Faculty of Science, University of Zagreb, Bijenička 32, HR-10000 Zagreb, Croatia*
[d]*Department of Chemistry, Faculty of Science, University of Zagreb, Horvatovac 102a, HR-10000 Zagreb, Croatia*

*Corresponding authors e-mail address:
jana.pisk@chem.pmf.hr (Jana Pisk), luka.pavic@irb.hr (Luka Pavić)

Highlights

- Glasses-(ceramics) from Na_2O-V_2O_5-(Al_2O_3)-P_2O_5-Nb_2O_5 system were evaluated for catalytic properties.
- Fatty acid decomposition was monitored using TG/DSC, TG-IR, and STA-QMS experiments.
- Dielectric properties were studied through solid-state impedance spectroscopy (SS-IS).
- Catalytic results and dielectric properties were correlated to observed structural features.
- The improvements in dielectric properties relate strongly with superior catalytic performance and increased V_2O_5 content.

Abstract

In the quest to mitigate greenhouse gas emissions, biofuels, particularly biodiesel, are compelling alternatives to fossil fuels due to their lower toxicity, renewability, biodegradability, lubricity, and cleaner combustion. This study explores cost-effective, innovative catalysts: glasses-(ceramics) derived from the Na_2O-V_2O_5-(Al_2O_3)-P_2O_5-Nb_2O_5 system, for the pyrolytic deoxygenation of long-chain fatty acids into alkanes. Thermogravimetric analysis/differential scanning calorimetry (TG/DSC) assessed catalytic activity, while TG-IR and STA-QMS provided insights into the catalytic mechanisms. Dielectric properties examined through solid-state impedance spectroscopy (SS-IS) revealed that increased V_2O_5 content enhances dielectric permittivity, dielectric strength, and dielectric loss, correlating with improved catalytic activity. Optimal properties were achieved with the highest V_2O_5 content, indicating potential applications in memory and switching devices and battery technology. This study highlights the versatility and multifunctionality of oxide glasses-(ceramics), enhanced through simple compositional adjustments.

Keywords: phosphate glasses, glass-ceramics, catalytic properties, dielectric properties, coupled TG-IR system, coupled STA-QMS system, impedance spectroscopy (IS)

Introduction

Climate change, the escalating energy demand, and the depletion of natural resources are pressing challenges of the 21st century. Biofuels offer a promising alternative to fossil fuels, potentially mitigating global greenhouse gas emissions. Among biofuels, biodiesel emerges as the most feasible substitute for petroleum diesel due to its lower toxicity, renewability, superior biodegradability, enhanced lubricity, and cleaner combustion characteristics in compression ignition engines [1].

The quality of biodiesel is intrinsically linked to the origin and composition of its feedstock, which typically includes vegetable oils, microalgae, cellulose, and waste agricultural sources [2]. Biodiesel is characterized by a higher cetane number than diesel fuel, absence of aromatics and virtually sulphur-free, containing 10 to 11 wt.% oxygen. These properties contribute to its ability to significantly reduce emissions of carbon monoxide, hydrocarbons, and particulate matter in exhaust gases when compared to petroleum-based diesel fuel. Biodiesel consists of mono-alkyl esters of long-chain fatty acids, primarily produced via the catalytic transesterification of triglycerides with short-chain alcohols under mild reaction conditions [3–8]. The typical alkyl fatty acid chains range from C10 to C22 esters of methanol or ethanol. The transesterification reaction presents significant challenges, including sensitivity to feedstock purity, the necessity of an effective catalyst to prevent saponification, and the complexity of the separation stage. Alternative methods include pyrolysis hydrotreating and deoxygenation reactions [9–14].

In recent years, research has focused extensively on developing high-performance deoxygenation catalysts, yielding significant advancements in the field. Notably, various metal catalysts (Pd, Pt, Ni, Rh, Ir, Ru, Os) supported on materials such as carbon, TiO_2, SiO_2, ZrO_2, and Al_2O_3 have been successfully developed for the deoxygenation of fatty acids [14–18]. Moreover,

the catalytic activity of the glass system V_2O_5-B_2O_3-P_2O_5 was evaluated through the oxidation of fatty acids [19,20]. Building on these advancements, we introduce an innovative concept: utilizing glasses-(ceramics) from the Na_2O-V_2O_5-(Al_2O_3)-P_2O_5-Nb_2O_5 system as catalysts for the deoxygenation of fatty acids (stearic, oleic and palmitic). The novelty of this approach is further enhanced by employing thermogravimetric analysis/differential scanning calorimetry (TG/DSC), along with coupled thermogravimetry-infrared spectroscopy (TG-IR) and simultaneous thermal analysis-quadrupole mass spectrometry (STA-QMS) experiments to monitor the reaction process, offering unprecedented insights into the catalytic mechanisms. To the best of our knowledge, this approach has not been previously reported, ensuring the originality of this investigation.

The oxide glasses-(ceramics) in this study are analyzed for their dielectric properties using solid-state impedance spectroscopy (SS-IS), revealing that dielectric permittivity (ε'), dielectric strength ($\Delta\varepsilon$), and dielectric loss (tan δ) increase with V_2O_5 content, correlating with enhanced catalytic activity. This relationship is similar to the one observed in the study of aluminosilicate clay minerals during catalytic cracking of cumene, attributed to their greater polarizability and higher permittivity, facilitating better substrate interaction and reaction [21]. Furthermore, the dielectric properties of the glasses-(ceramics) under study are noteworthy due to their potential in sodium-ion battery technology, acting as ionically conductive inorganic binders for solid-state electrolyte/electrode materials [22,23]. Their intrinsic ionic conductivity enhances ion transport, while higher dielectric constants improve ion dissociation and separation, boosting overall electrode and electrolyte performance [24]. With the introduction of vanadium, these materials may exhibit a mixed ionic-electronic electrical conductivity [25–27], where the electronic contribution arises from electron hopping via V^{4+}/V^{5+} redox pairs governed by the small polaron hopping (SPH) mechanism [28]. This opens new avenues for the use in memory and switching

devices [29], as well as in battery technology as cathode materials, [30–32] and as infrared transparent oxide glasses in photonic devices [33]. Our study of the Na_2O-V_2O_5-(Al_2O_3)-P_2O_5-Nb_2O_5 system confirms that oxide glasses-(ceramics) are versatile and easy-to-prepare materials with multifunctional capabilities, achieving enhanced dielectric and catalytic properties through simple compositional adjustments. Details regarding the experimental part (materials and methods) are given in Supplementary Information (SI).

Results and discussion

Stearic acid (SA) was selected as the model compound to optimize the measurement of the thermal decomposition of fatty acids (FAs), see **Figure S1 and Table S2 in SI**, and to investigate the influence of oxide glass-(ceramic) catalysts (CATs) on their thermal decomposition. Additional experiments were conducted on oleic acid (OA) and palmitic acid (PA) to elucidate the effects further. OA is unsaturated and contains 18 C atoms, while SA and PA are saturated and contain 18 and 16 C atoms, respectively. Under a nitrogen flow atmosphere, pure SA melts in the temperature range of 66–82 °C, and decomposes in a single step, with an onset temperature (T_{onset}) of 277 °C and an endset temperature (T_{endset},) of 322 °C (**Figure 1(a), Figure S2 and Table S3 in SI**), consistent with literature data [34–36]. The thermal decomposition data for OA and PA are provided in **Figures S3-S4 and Table S3 in SI**, demonstrating also good agreement with literature values [37,38].

Given that the selected glass-ceramic catalysts (CATs) for testing the thermal decomposition of fatty acids (FAs) contain varying proportions of V_2O_5 (up to 70 mol%), the subsequent phase of the study utilized commercially available V_2O_5 as the standard reference material. The mass loss associated with the decomposition of SA in the presence of V_2O_5 occurs

in four distinct steps. The first two decomposition steps, as indicated on the TG curve, correspond to two exothermic signals on the DSC curve at 279 °C and 317 °C, respectively. The subsequent two steps are accompanied by endothermic signals (**Figure 1(b)**). These exothermic signals are followed by significant mass losses of 23% and 10%, respectively, attributed to the SA decomposition in the presence of V_2O_5. Particularly, similar thermal behaviour has been reported for pure crystalline V_2O_5, where the exothermic signals were ascribed to the oxidation of VO_2 impurity to V_2O_5 and the recrystallization of V_2O_5 [39–43]. These processes cannot be excluded, suggesting that commercially available V_2O_5 may undergo changes upon interaction with SA during thermal treatment. Although addition of V_2O_5 significantly lowers the onset temperature of SA decomposition from 277 °C to 245 °C, the broader temperature range and more complex decomposition profile suggest that V_2O_5 adversely affects the thermal decomposition of SA.

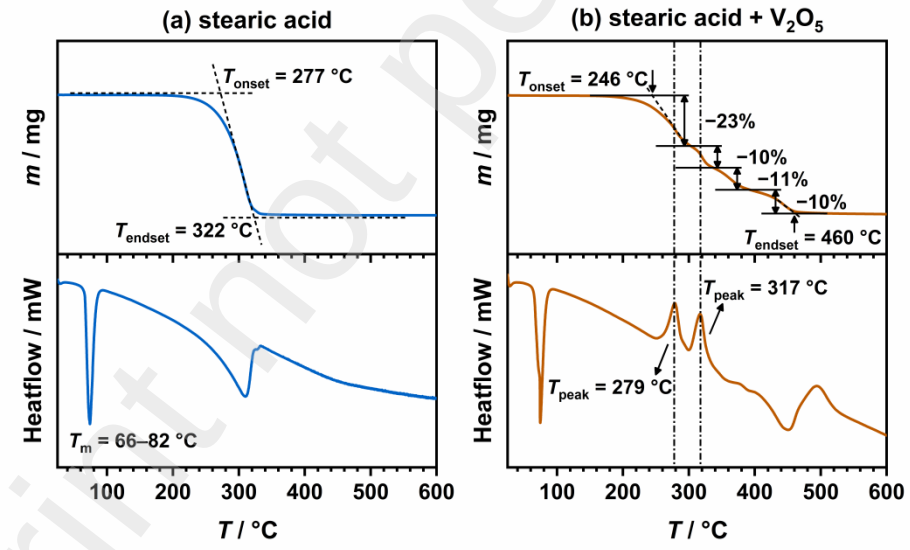

Figure 1. TG/DSC curves of the thermal decomposition of (a) pure stearic acid and (b) stearic acid mixed with V_2O_5 in a 1:1 ratio.

In contrast to pure V_2O_5, all glass-(ceramic) samples used as CATs mixed with SA in a 1:1 ratio exhibit a one-step weight loss (**Figure 2(a)**). Furthermore, the DSC curves for the prepared SA and CAT mixtures reveal no additional exothermic processes, indicating that the

decomposition of SA with CAT is akin to that of pure SA (**Figure S2 in SI**). This suggests that the tested glasses-(ceramics), wherein vanadium is arranged within the dominant V-based glass matrix, are potentially more reliable catalysts for the thermal decomposition of FAs than commercially available V_2O_5, as their addition does not result in complex decomposition process.

The thermal parameters of FA decomposition were determined from TG/DSC curves, and their variations in response to various CATs were analysed. The addition of these CATs to SA results in a shift of both onset and endset temperatures, T_{onset} and T_{endset}, of SA decomposition to lower values, with T_{onset} decreasing by 14–23 °C compared to that of pure SA (**Figure 2(b-d), Table S3 in SI**). A clear correlation between the thermal parameters and the V_2O_5 content in the glass-(ceramic) CATs is evident. Samples rich in V_2O_5 exhibit the most pronounced effects, as exemplified by the 70V-10P-20Na sample, which contains 70% V_2O_5, and significantly reduces the T_{onset} and T_{endset} of SA decomposition by 23 °C and 11 °C, respectively.

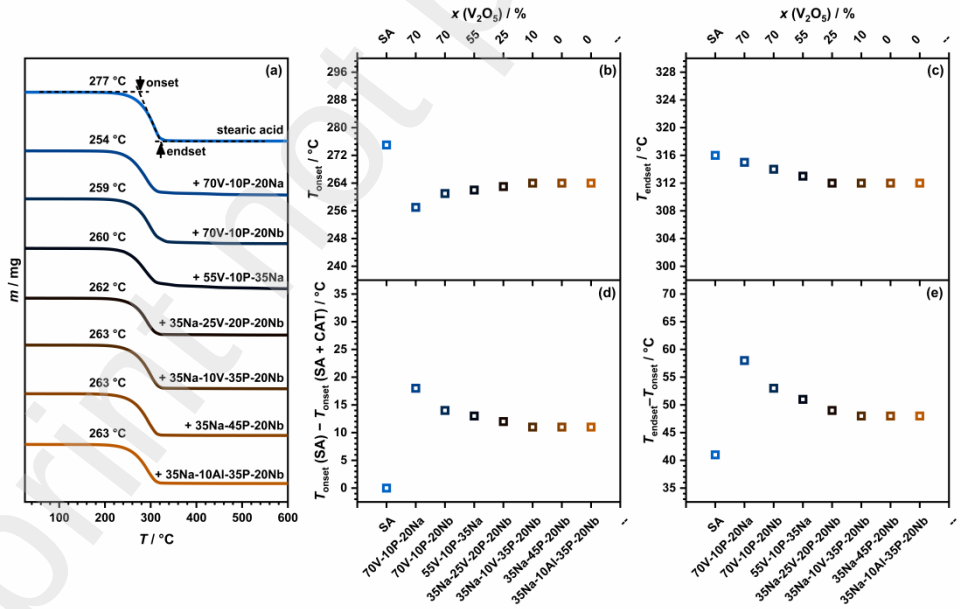

Figure 2. The influence of the addition of different glass-(ceramic) catalysts on: (a) TG curves of the thermal decomposition of stearic acid (SA), (b) the onset temperature, T_{onset}, (c) the endset temperature, T_{endset}, of the thermal decomposition of SA, the difference between (d) T_{onset} of the decomposition of SA and the SA mixed with the catalyst (CAT), T_{onset} (SA) − T_{onset} (SA + CAT), and (e) the endset and onset temperatures of decomposition, T_{endset} − T_{onset}, of SA.

Additionally, experiments performed using OA and PA as substrates exhibit a similar behaviour pattern as SA (**Figures S3-S5 and Table S3 in SI**) with T_{onset} shifting to lower values upon the addition of CATs. However, a somewhat narrower range of T_{onset} reduction is observed for these two FAs.

These findings are consistent with our prior publication, which highlighted the enhanced activity and selectivity of V_2O_5-rich glass-(ceramic) CATs [44]. While our earlier work focused on cyclooctene epoxidation reaction, the current study emphasises FA oxidation. The observed trend of increased activity in V_2O_5-rich glass-(ceramic) CATs is also reflected in their impact on the thermal decomposition of FA, underscoring the pivotal role of vanadium content in the catalytic activity of the studied glasses-(ceramics). Besides the proportion of V_2O_5 itself, the proportion of vanadium ions in the +4-oxidation state (electron configuration [Ar]$3d^1$), possessing a partially filled 3*d* orbital, might play a crucial role in the catalytic activity of the studied materials. Specifically, V^{4+} ions are present in the glass-(ceramic) because of redox equilibria in the glass melt, influenced by both the glass composition and the synthesis parameters. The V^{4+}/V_{total} ratio in samples containing V_2O_5, determined via EPR measurements, ranges from 3.4–20.5 % (**Table S1 in SI**), and the presence of V^{4+} ions could facilitate electron transfer from the substrate (FA) to the CAT [45], thereby possibly accelerating FA decomposition.

To overcome the limitations of TG/DSC in identifying degradation products, deeper insight into the thermal decomposition of FA with the addition of CAT was obtained through coupled TG-IR experiments. While pure SA shows only a slight increase in CO_2 signal intensity over time, the SA mixture with the 70V-10P-20Nb glass exhibits strong CO_2 signals that intensify notably as decomposition advances, indicating SA decarboxylation (**Figure 3, Figures S6-S7 in SI**). Moreover, pure SA shows a minimal decrease in the C=O bond signal intensity, indicating that

decomposition is just beginning: In contrast, the addition of CAT results in a significant decrease in the C=O bond signal over time, suggesting that SA decomposes at a lower temperature and that CAT accelerates its decomposition, a process that can be effectively monitored by IR spectroscopy. This observation is consistent with existing literature, highlighting the critical role of catalysts in achieving substantial conversion of SA and its decarboxylation to *n*-heptadecane. Conversely, SA without a catalyst undergoes decarboxylation to a minimal extent [16–18,46,47].

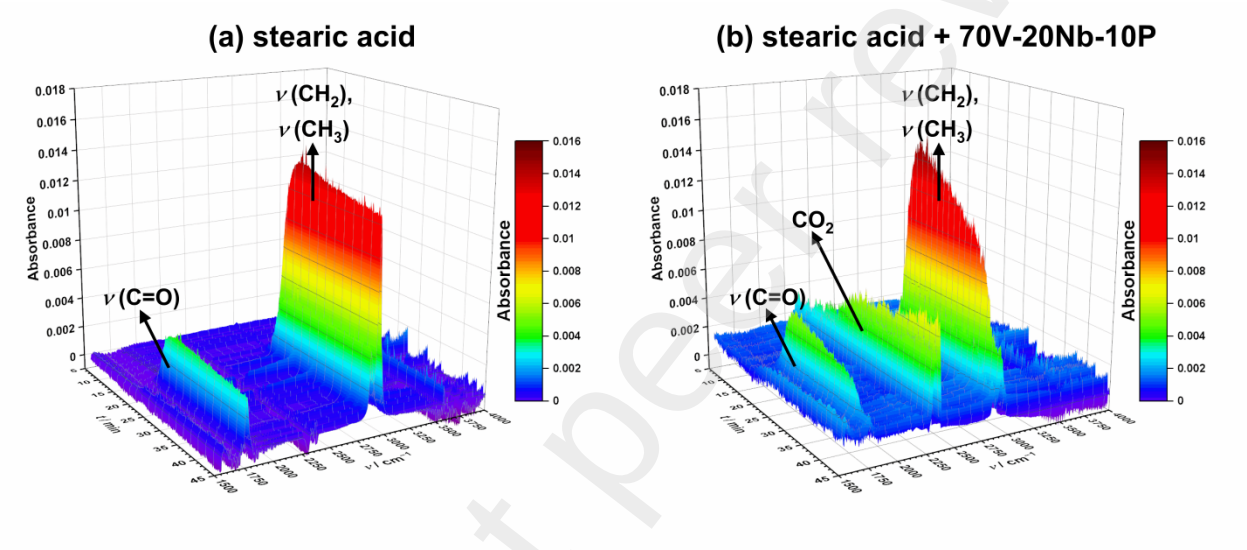

Figure 3. 3D colour maps showing the change in absorbance values of FT-IR spectra as a function of wavenumber, *v*, and time, *t*, for the thermal decomposition of (a) pure stearic acid and (b) stearic acid mixed with 70V-10P-20Nb sample.

Although the coupled TG-IR experiment could not detect a CO_2 signal for pure SA, likely due to instrument limitations given the low concentration of CO_2, the results of the coupled STA-QMS experiment confirm partial decarboxylation (**Figures S8-S9 in SI**). This is evident by the MS spectra of gaseous products showing characteristic signals for CO_2 at m/z = 12, 16, 28, and 44 (**Figure 4**). However, the stronger signal at m/z = 28 compared to m/z = 44 suggests that the decomposition of SA also involves a decarbonylation reaction, releasing CO, with the m/z = 28 signal attributed to a mixture of CO and CO_2. Moreover, the prominent signals at m/z = 17 and 18

correspond to H_2O and can be elucidated by the decomposition mechanism of SA [17]. This mechanism involves the release of water when two molecules of SA react to form stearic anhydride, and during the decarbonylation of SA to heptadecene (**Figure S9 in SI**).

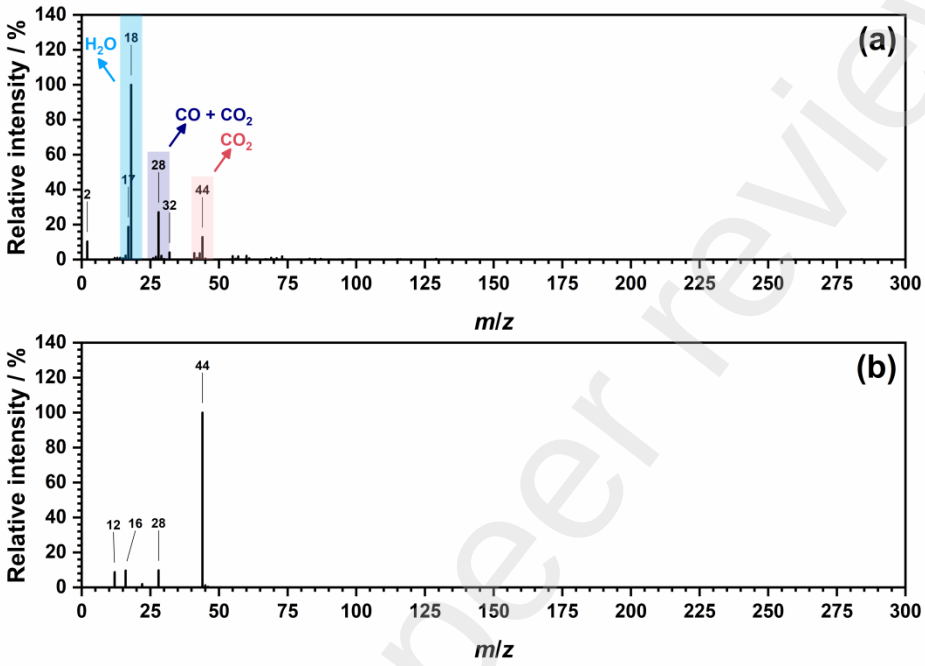

Figure 4. Comparison of (a) experimental MS spectrum of the thermal decomposition of stearic acid and (b) MS spectrum of CO_2.

A detailed analysis of the IR spectra collected during the thermal decomposition of SA, combined with the results of the coupled STA-QMS experiment, proposes that the resulting reaction mixtures likely consist of the starting material (SA), stearic anhydride (described in the literature as a reactive intermediate), along with *n*-heptadecane and CO_2 formed through the decarboxylation reaction (**Figure S7 in SI**), consistent with the proposed reaction mechanisms [16–18,46–48]. Nevertheless, since the bands corresponding to SA and *n*-heptadecane overlap, identifying the detected species via the IR method is challenging. Though, the strong CO_2 signal intensities, as previously mentioned, indicate improved SA conversion due to the catalytic effect of the 70V-10P-20Nb glass (**Figure S7(b) in SI**).

Alongside catalytic testing, the dielectric properties of all prepared samples were evaluated using Solid-State Impedance Spectroscopy (SS-IS). A detailed analysis of the complex permittivity (**Figures S10-S11 in SI**) and its scaling properties [49] (**Figure S12 in SI**) is provided in SI. The corresponding values of dielectric parameters, including dielectric permittivity, ε', dielectric strength, $\Delta\varepsilon$ [50], and dielectric loss, tan δ, are presented in **Table 1** and **Figure S13 in SI**. Dielectric parameters reach their highest values in V_2O_5-rich samples ($x(V_2O_5)$ = 70 mol%), declining with lower V_2O_5 content due to changes in glass composition, especially the reduced proportion of V_2O_5 and presence of less polarizable elements (Na, P, and O). It is worth mentioning that the highest dielectric parameters correlate with superior catalytic activity, exemplified by the 70V-10P-20Nb glass and 70V-10P-20Nb glass-ceramic achieving the most significant reduction in FA decomposition temperature. Drawing on insights from the study of the relationship between dielectric permittivity and the catalytic activity of aluminosilicate clay minerals in cumene cracking [21], it can be inferred that the higher proportion of highly polarizable V_2O_5 within the glass matrix of the studied glasses-(ceramics) similarly enhances catalyst reactivity toward FAs. This enhancement could occur by inducing polarization of weakly polar hydrocarbons, thereby augmenting their adsorption to the catalyst surface—an essential initial step in catalytic process.

Table 1. Dielectric permittivity, ε_∞, dielectric strength, $\Delta\varepsilon$, and loss factor, tan δ, for studied glasses-(ceramics).

Sample	ε_∞	$\Delta\varepsilon$ [a]	tanδ [a,b]
70V-10P-20Na	23.76	18.42	0.831
70V-10P-20Nb	29.76	20.45	0.739
55V-10P-35Na	27.91	101.37	0.074
35Na-25V-20P-20Nb	23.44	84.49	0.008
35Na-10V-35P-20Nb	17.47	43.46	0.019
35Na-45P-20Nb	15.20	34.29	0.066
35Na-10Al-35P-20Nb	18.31	46.69	0.030

[a]at T = 303 K
[b]at ν = 1 MHz

Conclusions

The research focuses on novel and cost-effective catalysts derived from the Na_2O-V_2O_5-(Al_2O_3)-P_2O_5-Nb_2O_5 glass-(ceramic) system for the decarboxylation of fatty acids (stearic, oleic, and palmitic acids) into long-chain alkanes, which are valuable compounds to produce new generation of biofuels. Comprehensive characterization techniques, including thermogravimetric analysis/differential scanning calorimetry (TG/DSC) coupled with infrared spectroscopy (TG-IR), and simultaneous thermal analysis-quadrupole mass spectrometry (STA-QMS), were utilized to elucidate the catalytic mechanisms, with a focus on stearic acid as a model substrate. To the best of our knowledge, the instrumentation and methodologies employed in this study represent a novel application in this field of research. The study also delves into the dielectric properties of these glasses-(ceramics) through solid-state impedance spectroscopy revealing that an increased V_2O_5 content significantly enhances dielectric permittivity, dielectric strength, and dielectric loss. These improvements in dielectric properties correlate strongly with superior catalytic performance and observed structural features. This research underscores the versatility and multifunctionality of oxide glasses-(ceramics), demonstrating that their properties can be finely tuned through compositional adjustments to meet specific technological demands.

Author Contributions

Conceptualisation: L. P., J. P.; Formal Analysis: S. M., Ž. S., P. M., L. K.; Investigation: S. M., P. M., L. K., Ž. S., L. P., J. P.; Methodology: L. P., J. P.; Visualization: S. M., L. P., J. P.; Validation: S. M., L. P., J. P.; Project administration: J. P., L. P.; Resources: J. P., L. P.; Supervision: J. P., L. P.; Funding acquisition: L. P., J. P.; Writing – original draft: S. M., L. P., J. P., Writing – review & editing: S. M., P. M., L. K., Ž. S., L. P., J. P.

Declaration of Competing Interest

The authors declare that they have no known competing financial interests or personal relationships that could have appeared to influence the work reported in this paper.

Acknowledgements

This work is supported by the Croatian Science Foundation, projects POLAR-ION-GLASS (IP-2018–01–5425) and "Young Researchers' Career Development Project – Training New Doctoral Students" (DOK-2021, S.M.). J.P. and Ž.S. acknowledge the support of project CiuK (Grant KK.01.1.1.02.0016) and CeNIKS (Grant No. KK.01.1.1.02.0013), respectively, co-financed by the Croatian Government and the European Union through the European Regional Development Fund-Competitiveness and Cohesion Operational Programme. This work is partially funded by the European Union – NextGenerationEU. Views and opinions expressed are however those of the author(s) only and do not necessarily reflect those of the European Union or the European Education and Culture Executive Agency (EACEA). Neither the European Union nor EACEA can be held responsible for them.

Supplementary materials

Supplementary material associated with this article can be found, in the online version, at doi:x.

References

[1] A. Srivastava, R. Prasad, Triglycerides-based diesel fuels, Renew. Sustain. Energy Rev. 4 (2000) 111–133. https://doi.org/10.1016/S1364-0321(99)00013-1.

[2] S. Lestari, P. Mäki-Arvela, J. Beltramini, G.Q.M. Lu, D.Yu. Murzin, Transforming Triglycerides and Fatty Acids into Biofuels, ChemSusChem 2 (2009) 1109–1119. https://doi.org/10.1002/cssc.200900107.

[3] A. Demirbaş, Biodiesel from vegetable oils via transesterification in supercritical methanol, Energy Convers. Manag. 43 (2002) 2349–2356. https://doi.org/10.1016/S0196-8904(01)00170-4.

[4] F. Ma, M.A. Hanna, Biodiesel production: a review1, Bioresour. Technol. 70 (1999) 1–15. https://doi.org/10.1016/S0960-8524(99)00025-5.

[5] H. Fukuda, A. Kondo, H. Noda, Biodiesel fuel production by transesterification of oils, J. Biosci. Bioeng. 92 (2001) 405–416. https://doi.org/10.1016/S1389-1723(01)80288-7.

[6] M. Hájek, A. Vávra, J. Mück, 2020. Butanol as a co-solvent for transesterification of rapeseed oil by methanol under homogeneous and heterogeneous catalyst. Fuel. 277, 118239. https://doi.org/10.1016/j.fuel.2020.118239.

[7] A.S. Ramadhas, S. Jayaraj, C. Muraleedharan, Use of vegetable oils as I.C. engine fuels—A review, Renew. Energy 29 (2004) 727–742. https://doi.org/10.1016/j.renene.2003.09.008.

[8] L. Petrus, M.A. Noordermeer, Biomass to biofuels, a chemical perspective, Green Chem. 8 (2006) 861–867. https://doi.org/10.1039/B605036K.

[9] P. Tamunaidu, S. Bhatia, Catalytic cracking of palm oil for the production of biofuels: Optimization studies, Bioresour. Technol. 98 (2007) 3593–3601. https://doi.org/10.1016/j.biortech.2006.11.028.

[10] G.W. Huber, P. O'Connor, A. Corma, Processing biomass in conventional oil refineries: Production of high quality diesel by hydrotreating vegetable oils in heavy vacuum oil mixtures, Appl. Catal. A Gen. 329 (2007) 120–129. https://doi.org/10.1016/j.apcata.2007.07.002.

[11] D. Kubička, P. Šimáček, N. Žilková, Transformation of Vegetable Oils into Hydrocarbons over Mesoporous-Alumina-Supported CoMo Catalysts, Top Catal 52 (2009) 161–168. https://doi.org/10.1007/s11244-008-9145-5.

[12] X. Yao, T.J. Strathmann, Y. Li, L.E. Cronmiller, H. Ma, J. Zhang, Catalytic hydrothermal deoxygenation of lipids and fatty acids to diesel-like hydrocarbons: a review, Green Chem. 23 (2021) 1114–1129. https://doi.org/10.1039/D0GC03707A.

[13] M. Tabandeh, C.K. Cheng, G. Centi, P.L. Show, W.-H. Chen, T.C. Ling, H.C. Ong, E.-P. Ng, J.C. Juan, S.S. Lam, 2022. Recent advancement in deoxygenation of fatty acids via homogeneous catalysis for biofuel production. Mol. Catal. 523, 111207. https://doi.org/10.1016/j.mcat.2020.111207.

[14] I. Kubičková, M. Snåre, K. Eränen, P. Mäki-Arvela, D.Yu. Murzin, Hydrocarbons for diesel fuel via decarboxylation of vegetable oils, Catal. Today 106 (2005) 197–200. https://doi.org/10.1016/j.cattod.2005.07.188.

[15] M. Snåre, I. Kubičková, P. Mäki-Arvela, K. Eränen, D.Yu. Murzin, Heterogeneous Catalytic Deoxygenation of Stearic Acid for Production of Biodiesel, Ind. Eng. Chem. Res. 45 (2006) 5708–5715. https://doi.org/10.1021/ie060334i.

[16] S.A.W. Hollak, J.H. Bitter, J. van Haveren, K.P. de Jong, D.S. van Es, Selective deoxygenation of stearic acid via an anhydride pathway, RSC Adv. 2 (2012) 9387–9391. https://doi.org/10.1039/C2RA21651E.
[17] W. Li, Y. Gao, S. Yao, D. Ma, N. Yan, Effective deoxygenation of fatty acids over Ni(OAc)2 in the absence of H2 and solvent, Green Chem. 17 (2015) 4198–4205. https://doi.org/10.1039/C5GC01147G.
[18] B. Chen, Z. Zhou, Y. Li, K.B. Tan, Y. Wang, X. Rao, J. Huang, X. Zhang, Q. Li, G. Zhan, 2023. Catalytic pyrolysis of fatty acids and oils into liquid biofuels and chemicals over supported Ni catalysts on biomass-derived carbon. Appl. Catal. B: Environ. 338, 123067. https://doi.org/10.1016/j.apcatb.2023.123067.
[19] S.-Y. Choi, B.-K. Ryu, Nanocrystallization of vanadium borophosphate glass for improving the electrical and catalytic properties, J. Nanomaterials 2015 (2015) 1–9. https://doi.org/10.1155/2015/201597.
[20] S.-Y. Choi, B.-K. Ryu, Effects of crystallization on the structural, electrical, and catalytic properties of 75V2O5–15B2O3–10P2O5 glass, J. Non-Cryst. Solids 431 (2016) 112–117. https://doi.org/10.1016/j.jnoncrysol.2015.05.009.
[21] B. Hanna, F.H. Khalil, Relation between the electric properties and the catalytic activity of some Egyptian clays, Surface Technology 17 (1982) 61–68. https://doi.org/10.1016/0376-4583(82)90061-9.
[22] T. Honma, M. Okamoto, T. Togashi, N. Ito, K. Shinozaki, T. Komatsu, Electrical conductivity of Na2O–Nb2O5–P2O5 glass and fabrication of glass–ceramic composites with NASICON type Na3Zr2Si2PO12, Solid State Ion. 269 (2015) 19–23. https://doi.org/10.1016/j.ssi.2014.11.009.
[23] S. Trivedi, V. Pamidi, M. Fichtner, M.A. Reddy, Ionically conducting inorganic binders: a paradigm shift in electrochemical energy storage, Green Chem. 24 (2022) 5620–5631. https://doi.org/10.1039/D2GC01389D.
[24] L.-Z. Fan, H. He, C.-W. Nan, Tailoring inorganic–polymer composites for the mass production of solid-state batteries, Nat Rev Mater 6 (2021) 1003–1019. https://doi.org/10.1038/s41578-021-00320-0.
[25] M. Wasiucionek, J. Garbarczyk, P. Kurek, W. Jakubowski, Electrical properties of glasses of the Na_2O-V_2O_5-P_2O_5 system, Solid State Ion. 70–71 (1994) 346–349. https://doi.org/10.1016/0167-2738(94)90334-4.
[26] M.C. Ungureanu, M. Lévy, J.L. Souquet, Mixed conductivity of glasses in the P_2O_5-V_2O_5-Na_2O system, Ionics 4 (1998) 200–206. https://doi.org/10.1007/BF02375946.
[27] S. Marijan, T. Klaser, M. Mirosavljević, P. Mošner, L. Koudelka, Ž. Skoko, J. Pisk, L. Pavić, 2024. Exploring the Effect of V_2O_5 and Nb_2O_5 Content on the Structural, Thermal, and Electrical Characteristics of Sodium Phosphate Glasses and Glass–Ceramics. Int. J. Mol. Sci. 25, 3005. https://doi.org/10.3390/ijms25053005.
[28] I.G. Austin, N.F. Mott, Polarons in crystalline and non-crystalline materials, Advances in Physics 18 (1969) 41–102. https://doi.org/10.1080/00018736900101267.
[29] C. Narayana Reddy, S. Asokan, R.V. Anavekar, High field electrical behaviour in lithium-phospho-vanadate glass system, Bull. Mater. Sci. 30 (2007) 65–68. https://doi.org/10.1007/s12034-007-0011-z.
[30] M. Kindle, Y. Cha, J.S. McCloy, M.-K. Song, Alternatives to Cobalt: Vanadate Glass and Glass-Ceramic Structures as Cathode Materials for Rechargeable Lithium-Ion Batteries,

ACS Sustain. Chem. Eng. 9 (2021) 629–638. https://doi.org/10.1021/acssuschemeng.0c04026.
[31] A. Ibrahim, S. Watanabe, M. Razum, L. Pavić, Z. Homonnay, E. Kuzmann, M.Y. Hassaan, S. Kubuki, 2023. Structural, Electrical, and Electrochemical Properties of a Na_2O-V_2O_5 Ceramic Nanocomposite as an Active Cathode Material for a Na-Ion Battery. Crystals. 13, 1521. https://doi.org/10.3390/cryst13101521.
[32] S. Petnikota, R. Chua, Y. Zhou, E. Edison, M. Srinivasan, 2018. Amorphous Vanadium Oxide Thin Films as Stable Performing Cathodes of Lithium and Sodium-Ion Batteries. Nanoscale Res. Lett. 13, 363. https://doi.org/10.1186/s11671-018-2766-0.
[33] A. Shearer, B. Hauke, M. Montazerian, J.C. Mauro, 2023. A critical review of infrared transparent oxide glasses. Opt. Mater.: X. 20, 100258. https://doi.org/10.1016/j.omx.2023.100258.
[34] S. Niu, H. Yu, S. Zhao, X. Zhang, X. Li, K. Han, C. Lu, Y. Wang, Apparent kinetic and thermodynamic calculation for thermal degradation of stearic acid and its esterification derivants through thermogravimetric analysis, Renew. Energy 133 (2019) 373–381. https://doi.org/10.1016/j.renene.2018.10.045.
[35] R.P. Shepardson, E.A. Bazilevskaya, K.J. Harvatine, Physical characterization of fatty acid supplements with varying enrichments of palmitic and stearic acid by differential scanning calorimetry, J. Dairy Sci. 103 (2020) 8967–8975. https://doi.org/10.3168/jds.2019-18131.
[36] W. Li, X. Zhang, R. Liu, S. Xu, S. Xu, Y. Lan, Y. Fu, Y. Zhang, Y. Feng, W. Cao, 2023. Thermal decomposition, flame propagation, and combustion reactions behaviours of stearic acid by experiments and molecular dynamic simulation. Chem.Eng. J. 461, 141906. https://doi.org/10.1016/j.cej.2023.141906.
[37] S. Niu, Y. Zhou, H. Yu, C. Lu, K. Han, Investigation on thermal degradation properties of oleic acid and its methyl and ethyl esters through TG-FTIR, Energy Convers. Manag. 149 (2017) 495–504. https://doi.org/10.1016/j.enconman.2017.07.053.
[38] B. Wu, Y. Zhao, Q. Liu, C. Zhou, X. Zhang, J. Lei, Form-stable phase change materials based on castor oil and palmitic acid for renewable thermal energy storage, J. Therm. Anal. Calorim. 137 (2019) 1225–1232. https://doi.org/10.1007/s10973-019-08041-x.
[39] C. Zheng, X. Zhang, Z. Qiao, D. Lei, Preparation and Characterization of Nanocrystal V_2O_5, J. Solid State Chem. 159 (2001) 181–185. https://doi.org/10.1006/jssc.2001.9148.
[40] Y. Chen, H. Liu, W.-L. Ye, Preparation and electrochemical properties of submicron spherical V_2O_5 as cathode material for lithium ion batteries, Scripta Materialia 59 (2008) 372–375. https://doi.org/10.1016/j.scriptamat.2008.04.009.
[41] R. Abazari, S. Sanati, L.A. Saghatforoush, Non-aggregated divanadium pentoxide nanoparticles: A one-step facile synthesis. Morphological, structural, compositional, optical properties and photocatalytic activities, Chem. Eng. J. 236 (2014) 82–90. https://doi.org/10.1016/j.cej.2013.09.056.
[42] M. Prześniak-Welenc, M. Łapiński, T. Lewandowski, B. Kościelska, L. Wicikowski, W. Sadowski, 2015. The Influence of Thermal Conditions on V_2O_5 Nanostructures Prepared by Sol-Gel Method. J.Nanomaterials. 2015, 418024. https://doi.org/10.1155/2015/418024.
[43] D. Govindarajan, V. Uma Shankar, R. Gopalakrishnan, Supercapacitor behavior and characterization of RGO anchored V_2O_5 nanorods, J. Mater. Sci: Mater. Electron 30 (2019) 16142–16155. https://doi.org/10.1007/s10854-019-01984-9.

[44] J. Pisk, S. Marijan, T. Klaser, P. Mošner, L. Koudelka, D. Agustin, Ž. Skoko, L. Pavić, 2024. Peculiar catalytic properties of oxide glass-(ceramics) in epoxidation reactions. J.Non-Cryst.Solids. 626, 122780. https://doi.org/10.1016/j.jnoncrysol.2023.122780.
[45] Y. Zhang, N. Wang, Y. Huang, W. Wu, C. Huang, C. Meng, Fabrication and catalytic activity of ultra-long V_2O_5 nanowires on the thermal decomposition of ammonium perchlorate, Ceram. Int. 40 (2014) 11393–11398. https://doi.org/10.1016/j.ceramint.2014.03.026.
[46] K.D. Maher, K.M. Kirkwood, M.R. Gray, D.C. Bressler, Pyrolytic Decarboxylation and Cracking of Stearic Acid, Ind. Eng. Chem. Res. 47 (2008) 5328–5336. https://doi.org/10.1021/ie0714551.
[47] Y. Zhang, C. Zhang, W. Li, Q. Xiao, F. Jiao, S. Xu, Y. Lan, Y. Fu, C.-M. Shu, W. Cao, 2023. Reaction mechanism of stearic acid pyrolysis via reactive molecular dynamics simulation and TG-IR technology. Renew. Energy. 217, 119115. https://doi.org/10.1016/j.renene.2023.119115.
[48] A.-J. Dong, J.-W. Zhang, K. Jiang, L.-D. Deng, Characterization and in vitro degradation of poly(octadecanoic anhydride), J. Mater. Sci. Mater. Med. 19 (2008) 39–46. https://doi.org/10.1007/s10856-007-3166-7.
[49] B. Roling, Scaling properties of the conductivity spectra of glasses and supercooled melts, Solid State Ion. 105 (1998) 185–193. https://doi.org/10.1016/S0167-2738(97)00463-3.
[50] D.L. Sidebottom, Universal Approach for Scaling the ac Conductivity in Ionic Glasses, Phys. Rev. Lett. 82 (1999) 3653–3656. https://doi.org/10.1103/PhysRevLett.82.3653.